Isoscalar and isovector dipole strength distributions in nuclei and the Schiff moment

N. Auerbach*
School of Physics and Astronomy, Tel Aviv University, Tel Aviv 69978, Israel
and Department of Physics and Astronomy, Michigan State University, East Lansing, Michigan 48824, USA

Ch. Stoyanov†
Institute for Nuclear Research and Nuclear Energy, Bulgarian Academy of Science, Sofia, Bulgaria

M. R. Anders‡ and S. Shlomo§
Cyclotron Institute, Texas A&M University, College Station, Texas 77843, USA
(Received 24 October 2013; revised manuscript received 10 December 2013; published 31 January 2014)

It was pointed out that the isoscalar dipole strength distribution in nuclei contributes to the Schiff moment. The nuclear Schiff moment is essential in the mechanism that induces parity and time-reversal violations in the atom. In this paper, we explore, theoretically, the properties and systematics of the isoscalar dipole in nuclei with an emphasis on the low-energy strength and the inverse energy-weighted sum which determines the Schiff moment. We also study the influence of the isovector dipole strength distribution on the Schiff moment. The influence of large neutron excess in exotic nuclei is examined. The centroid energies of the isoscalar giant dipole resonance and the overtone of the isovector giant dipole resonance are given for a wide range of nuclei.

DOI: 10.1103/PhysRevC.89.014335 PACS number(s): 21.60.Ev, 21.60.Jz, 24.30.Cz, 24.80.+y

I. INTRODUCTION

The study of giant resonances is not new in nuclear physics. However, there is continuous research on this subject as new resonances are found and new properties of the resonances are discovered. Moreover, it is now clear that many of the resonances play an important role in determining the properties of nuclear structures and reactions and contribute to the understanding of nuclear phenomena. For example, a whole class of isovector giant resonances helps in the study of symmetry energy, the determination of isospin mixing, etc. In a recent paper [1], it was pointed out that the isoscalar dipole (ISD) resonance [2] could have a substantial contribution to the nuclear Schiff moment whose operator is the same as the operator commonly used in the study of the ISD strength distribution. In this paper, we also consider the influence of the isovector dipole (IVD) strength distribution on the Schiff moment. The value of the Schiff moment is central to the measurement of time-reversal violation in an atom [3,4]. One of the novelties in the study of nuclear resonances is the realization that some of the resonances have significant strength concentrated at lower energies, away from the main peak. These are referred to as the "pygmy resonances." It has been known for a long time that the ISD and the IVD have low-lying strength, around 10 MeV of the excitation energy, in many spherical nuclei [5–12]. This means that the inverse energy-weighted sum (IEWS) of the strength distribution is particularly enhanced. The mechanism considered in Ref. [1] finds that the Schiff moment in odd-even nuclei *is proportional to the IEWS of the ISD* in the even-even core and, therefore, the Schiff moment is quite large when the contribution of the ISD is included. The odd nucleon couples to the 0^+ ground state and to the 1^- dipole strength. States with the same angular momentum J, but opposite parity, mix via an assumed time-reversal and parity-violating interaction. As a result, one finds a nonzero Schiff moment. That Schiff moment induces in the atom parity and time-reversal mixing which, in turn, produces a static electric dipole moment of the atom which is measured in experiment [13]. As mentioned above, one derives an expression for the static Schiff moment that depends linearly on the inverse energy-weighted sum of the ISD *strength* in the even core (see Eq. (37) in Ref. [1]). In the above reference, it was conjectured that some of the ISD strength in exotic nuclei with large neutron excess and in deformed nuclei might move to even lower energies by enhancing the IEWS and, thus, the Schiff moment.

The commonly used operator for the ISD is defined as [1,2]

$$\mathbf{D} = \sum_i \left(r_i^2 - \frac{5}{3}\langle r^2 \rangle \right) \boldsymbol{r}_i , \tag{1}$$

whereas, *the isoscalar* part of the Schiff operator is defined as [3,4]

$$\mathbf{S} = \frac{1}{10} \sum_i \left(r_i^2 - \frac{5}{3}\langle r^2 \rangle \right) \boldsymbol{r}_i . \tag{2}$$

Thus, the two operators, apart from normalization, are the same. The Schiff moment is the ground-state expectation value of the Schiff operator in an odd-even nucleus in the presence of a time-reversal-violating interaction [1]. Hence, extensive research on the ISD strength distribution will have an impact on the study of the Schiff moments in nuclei. There is also the *isovector* part of the Schiff operator, which is given by Eq. (2) multiplied by the isospin operator t_{zi}. In this paper, we will also consider the influence of the IVD strength distribution and of the neutron excess on the *isovector part* of the Schiff moment. This aspect was not treated explicitly in the past.

*auerbach@post.tau.ac.il
†cpstoyanov@gmail.com
‡manders14@neo.tamu.edu
§shlomo@comp.tamu.edu

Here, we should stress the following point. The Schiff strength distribution that we discuss in this paper is related to the even-even nucleus. The Schiff moment that is relevant to the measurement of the static atomic dipole moment is the one that is present in the odd-even nucleus. To determine this moment, one has to introduce the weak time-reversal-violating interaction. In Ref. [1], it was shown that, when the ISD strength distribution is taken into account, the Schiff moment in the odd-even nucleus is proportional to the inverse energy-weighted sum of the ISD in the even-even nucleus. The same also is true for the isovector Schiff moment, however, as shown in Ref. [1], the isovector part of the Schiff moment has other contributions that are not proportional to the *strength* of the IVD but involve the amplitudes of the IVD. Therefore, when considering the IVD strength contribution to the atomic dipole measurements, one should keep this in mind. Apart from the role played by the ISD and the IVD strength distributions in the calculation of the nuclear Schiff moment, there is a general interest in the properties of the isoscalar giant dipole resonance (ISGDR) and the overtone of the isovector giant dipole resonance (OIVGDR) and, in particular, in the low-energy components the ISD and IVD strength distributions. In the next two sections, we present a theoretical study of the ISD and the IVD strength distributions in spherical nuclei.

II. THEORETICAL FORMULATION

We have carried out calculations within the Hartree-Fock-(HF-) based random-phase approximation (RPA) for the strength distributions of the ISD and IVD in a wide range of nuclei.

A. Skyrme-type interaction

In our HF-based RPA calculations, we have adopted the following form for the Skyrme-type effective nucleon-nucleon interaction [14]:

$$\begin{aligned} V_{12} &= t_0\left(1+x_0P_{12}^{\sigma}\right)\delta(\vec{r}_1-\vec{r}_2) \\ &+\frac{1}{2}t_0\left(1+x_1P_{12}^{\sigma}\right)\left[\overleftarrow{k}_{12}^{2}\ \delta(\vec{r}_1-\vec{r}_2)+\delta(\vec{r}_1-\vec{r}_2)\vec{k}_{12}^{2}\right] \\ &+t_2\left(1+x_2P_{12}^{\sigma}\right)\overleftarrow{k}_{12}\delta(\vec{r}_1-\vec{r}_2)\vec{k}_{12} \\ &+\frac{1}{6}t_3\left(1+x_3P_{12}^{\sigma}\right)\rho^{\alpha}\left(\frac{\vec{r}_1+\vec{r}_2}{2}\right)\delta(\vec{r}_1-\vec{r}_2) \\ &+iW_0\overleftarrow{k}_{12}\delta(\vec{r}_1-\vec{r}_2)(\vec{\sigma}_1+\vec{\sigma}_2)\times\vec{k}_{12}, \end{aligned} \tag{3}$$

where t_i, x_i, α, and W_0 are the parameters of the interaction, P_{12}^{σ} is the spin-exchange operator, $\vec{\sigma}_i$ is the Pauli spin operator, $\vec{k}_{12}=-i(\vec{\nabla}_1-\vec{\nabla}_2)/2$, and $\overleftarrow{k}_{12}=-i(\overleftarrow{\nabla}_1-\overleftarrow{\nabla}_2)/2$. Here, the right and left arrows indicate that the momentum operators act on the right and on the left, respectively. The corresponding HF single-particle potential $V_{\rm HF}$ and the total energy E of the system are given by

$$V_{\rm HF}=\frac{\delta H}{\delta\rho},\quad E=\int H(r)d^3r, \tag{4}$$

respectively, where $H(r)$ is the Skyrme energy-density functional (EDF) [15], obtained by using Eq. (3).

B. HF-RPA calculations of strength functions

In this paper, we have carried out fully self-consistent HF-based RPA calculations of the strength distributions of the electric isoscalar and isovector dipole excitations in a wide range of spherical nuclei by employing commonly used effective Skyrme-type interactions of the form of Eq. (3) and by adopting the numerical method for RPA described in Refs. [15–19]. It is formulated in terms of coordinatelike Q (time-even) and momentumlike P (time-odd) particle-hole (p-h) operators and is adapted for a given EDF. We point out that, to ensure self-consistency, we have carried out the calculations by using a large p-h space and have included all the terms of the p-h residual interaction (time-even and time-odd) which are associated with the EDF used in the HF calculations. No additional time-odd residual interactions were added. For a given probing operator F_L, we have calculated the strength function,

$$S(E)=\sum_j|\langle 0|F_L|j\rangle|^2\delta(E_j-E_0). \tag{5}$$

Here, $|0\rangle$ is the RPA ground state, and the sum is over all RPA excited states $|j\rangle$ with the corresponding excitation energies E_j. We adopt the single-particle scattering operator,

$$F_L=\sum_{iM}f(r_i)Y_{LM}(i), \tag{6}$$

for isoscalar ($T=0$) excitations and

$$F_L=\frac{Z}{A}\sum_{nM}f(r_n)Y_{LM}(n)-\frac{N}{A}\sum_{pM}f(r_p)Y_{LM}(p) \tag{7}$$

for isovector excitations ($T=1$). We then determine the energy moments of the strength function,

$$m_k=\int_0^{\infty}E^kS(E)dE. \tag{8}$$

The centroid energy $E_{\rm CEN}$ then is obtained from

$$E_{\rm CEN}=\frac{m_1}{m_0}. \tag{9}$$

The energy moment m_1 can also be calculated by using the HF ground-state wave function, thereby leading to an energy-weighted sum rule (EWSR) [20,21]. For the isoscalar F_L in Eq. (6), the EWSR is given by

$$m_1(L,T=0)=\frac{1}{4\pi}\frac{\hbar^2}{2m}(2L+1)\int g_L(r)\rho(r)4\pi r^2dr, \tag{10}$$

where $\rho(r)$ is the HF ground-state matter density distribution and

$$g_L(r)=\left(\frac{df}{dr}\right)^2+L(L+1)\left(\frac{f}{r}\right)^2. \tag{11}$$

For the isovector ($T=1$) operator F_L of Eq. (7), the EWSR is given by

$$m_1(L,T=1)=\frac{NZ}{A^2}m_1(L,T=0)[1+\kappa-\kappa_{np}], \tag{12}$$

where κ is the enhancement factor which is due to the momentum dependence of the effective nucleon-nucleon interaction

and is given by

$$\kappa = \frac{(1/2)[t_1(1+x_1/2)+t_2(1+x_2/2)]}{(\hbar^2/2m)(4NZ/A^2)} \times \frac{2\int g_L(r)\rho_p(r)\rho_n(r)4\pi r^2 dr}{\int g_L(r)\rho(r)4\pi r^2 dr}, \quad (13)$$

where t_i and x_i are the parameters of the Skyrme interaction. The correction κ_{np}, which arises because of the difference in the profiles of the neutron and proton density distributions [i.e., because $\rho_n(r) - \rho_p(r) \neq \frac{N-Z}{A}\rho(r)$], is given by

$$\kappa_{np} = \frac{(N-Z)}{A}\frac{A}{NZ}\frac{\int g_L(r)[Z\rho_n(r) - N\rho_p(r)]4\pi r^2 dr}{\int g_L(r)\rho(r)4\pi r^2 dr}. \quad (14)$$

In the results presented in this paper, for the isoscalar dipole ($T = 0$, $L = 1$), we use the probing operator of Eq. (6) with

$$f(r) = r^3 - (5/3)\langle r\rangle^2 r, \quad (15)$$

which is proportional to the Schiff operator [see Eqs. (1) and (2)]. For the isovector dipole ($T = 1$, $L = 1$), we use the probing operator of Eqs. (7) and (15) and not the usual operator linear in r. Note, for the ISD, the second term in $f(r)$ is added to ensure zero contribution from the spurious state, associated with the center-of-mass motion, which has a transition density of the form $d\rho/dr$ [22,23]. We note that, in the Goldhaber-Teller model for the IVGDR, the transition density has the form of $d\rho/dr$ and, therefore, there is no contribution to the strength function of the operator $f(r) = r^3 - (5/3)\langle r\rangle^2 r$ from the IVGDR. In a microscopic HF-based RPA calculation, the form of the IVGDR transition density is close to $d\rho/dr$, and thus, we only expect a small contribution to the strength function of the IVD associated with $f(r)$ from the region of the IVGDR.

We have carried out fully self-consistent HF-based RPA. We add that, in our calculations, the EWSRs, Eq. (12), are fulfilled within better than 1% and, for the ISD, the spurious state appears at excitation energies below 0.2 MeV.

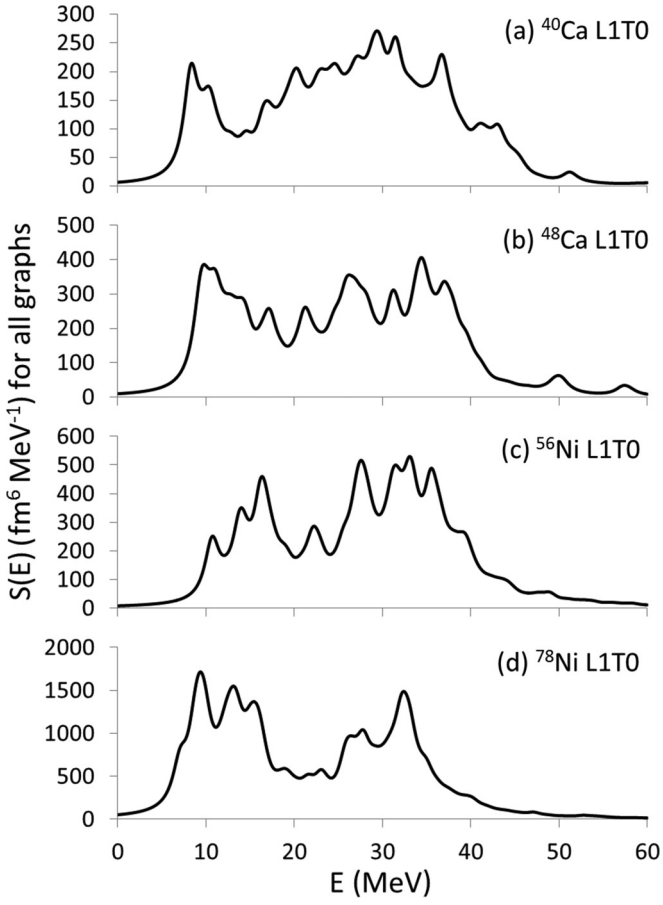

FIG. 1. Self-consistent HF-based RPA results for the distribution of the strength function $S(E)$ of the isoscalar dipole, obtained by using the probing operator of Eqs. (6) and (15) for the ^{40}Ca, ^{48}Ca, ^{56}Ni, and ^{78}Ni nuclei, calculated by using the KDE0v1 Skyrme interaction [25]. An excitation energy range of 0–60 MeV and a Lorenzian smearing of a 2-MeV width were used in the calculation.

III. RESULTS

We now present results of the HF-based RPA calculations of the strength distribution $S(E)$, the strength function divided by the energy $S(E)/E$, and the inverse energy-weighted sum of the strength distribution m_{-1} of the ISD for a wide range of nuclei. For the IVD, we only present the results for $S(E)$ and m_{-1}. We should stress that the reason we present the inverse

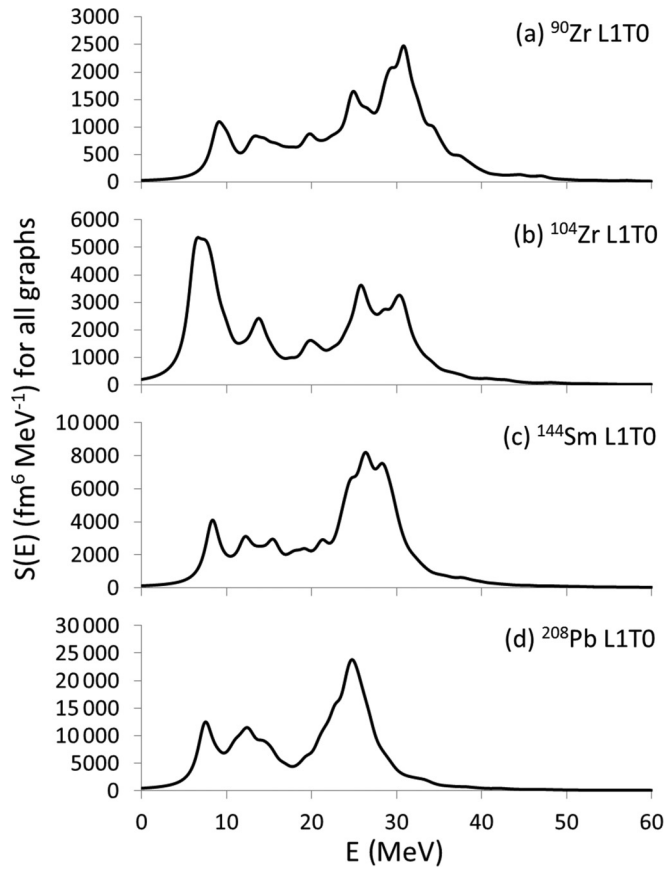

FIG. 2. Same as Fig. 1 but for the ^{90}Zr, ^{104}Zr, ^{144}Sm, and ^{208}Pb nuclei.

energy-weighted strength distribution, in addition to the strength distribution, is the fact the Schiff moment depends on the inverse energy-weighted sum [1,4]. We are concentrating on the low-energy region where the $S(E)/E$ is large. We also include results for the centroid energies of the ISGDR and the overtone of the OIVGDR. The calculations were carried out for 18 frequently used Skyrme-type interactions (see Ref. [16]): SGII [24], KDE0 [25], KDE0v1 [25], SKM* [26], SK255 [27], SkI3 [28], SkI4 [28], SkI5 [28], SV-bas [29], SV-min [29], SV-m56-O [30], SV-m64-O [30], SLy4 [31], SLy5 [31], SLy6 [31], SkMP [32], SkP [33], and SkO′ [34]. These interactions are associated with the ranges of values of symmetric nuclear matter (NM) properties (see Ref. [16]): The binding energy per nucleon is $E/A = 15.56$–16.33 MeV, the saturation density is $\rho_0 = 0.156 - 0.165$ fm^{-3}, the incompressibility coefficient is $K_{\rm NM} = 201$–258 MeV, the symmetry energy coefficient is $J = 26.80$–37.40 MeV, the coefficients related to the slope and curvature of the symmetry energy at the saturation density of $L = 31$–129 MeV, $K_{\rm sym} = -267$–160 MeV, respectively, the effective mass is $m^*/m = 0.56$–1.00, and the enhancement coefficient in the energy EWSR of the IVGDR is $\kappa = 0.08$–0.71.

By using the probing operator of Eqs. (6) and (15), in Figs. 1 and 2, we present the HF-based RPA results for the strength function $S(E)$ of the ISD in ^{40}Ca, ^{48}Ca, ^{56}Ni, and ^{78}Ni (Fig. 1) and in ^{90}Zr, ^{104}Zr, ^{144}Sm, and ^{208}Pb (Fig. 2), calculated by using the KDE0v1 Skyrme interaction [25] that is representative of the strength distributions for the rest of the interactions. Note the strong enhancement in the ISD strength distributions at low energy in the neutron-rich nuclei.

In Figs. 3 and 4, we show the HF-based RPA results for the strength function $S(E)$ of the IVD, obtained by using the probing operator of Eqs. (7) and (15) in ^{40}Ca, ^{48}Ca, ^{56}Ni, and ^{78}Ni (Fig. 3) and in ^{90}Zr, ^{104}Zr, ^{144}Sm, and ^{208}Pb (Fig. 4) calculated by using the KDE0v1 Skyrme interaction [25]. Note the low strength in the region of the IVGDR, which should vanish for a transition density of the form of $d\rho/dr$. Also note the scale of the strength function compared to the corresponding strength of the ISD.

In Figs. 5 and 6, we display the HF-based RPA results for the strength function divided by the energy, $S(E)/E$, of the ISD, obtained by using the probing operator of Eqs. (6) and (15), in ^{40}Ca, ^{48}Ca, ^{56}Ni, and ^{78}Ni (Fig. 5) and in ^{90}Zr, ^{104}Zr, ^{144}Sm, and ^{208}Pb (Fig. 6) calculated by using the KDE0v1 Skyrme interaction [25]. Note the relatively large contribution to the moment m_{-1} from the low-energy region, in particular, in the case of neutron-rich nuclei.

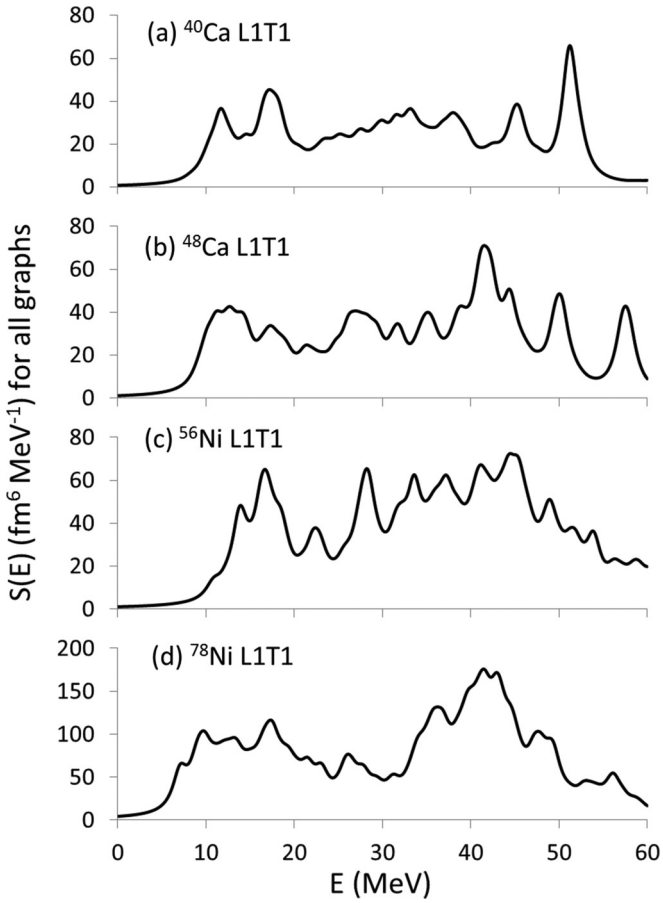

FIG. 3. Same as Fig. 1 but for the IVD with the probing operator of Eqs. (7) and (15).

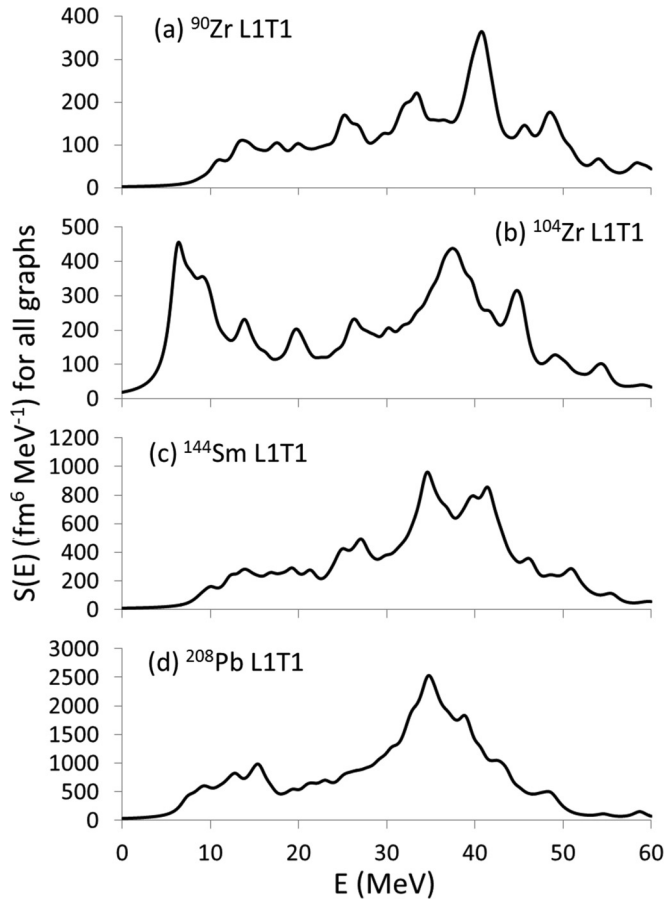

FIG. 4. Same as Fig. 2, but for the IVD with the probing operator of Eqs. (7) and (15).

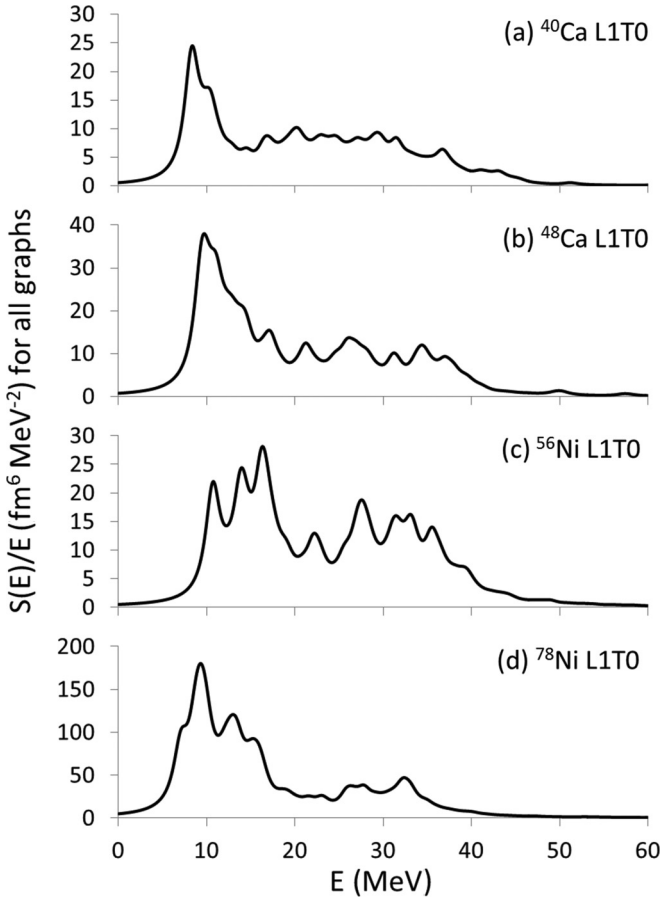

FIG. 5. Self-consistent HF-based RPA results for the distribution of the strength function divided by the energy, $S(E)/E$, of the isoscalar dipole, obtained by using the probing operator of Eqs. (6) and (15) for the ^{40}Ca, ^{48}Ca, ^{56}Ni, and ^{78}Ni nuclei, calculated by using the KDE0v1 Skyrme interaction [25]. An excitation energy range of 0–60 MeV and a Lorenzian smearing of a 2-MeV width were used in the calculation.

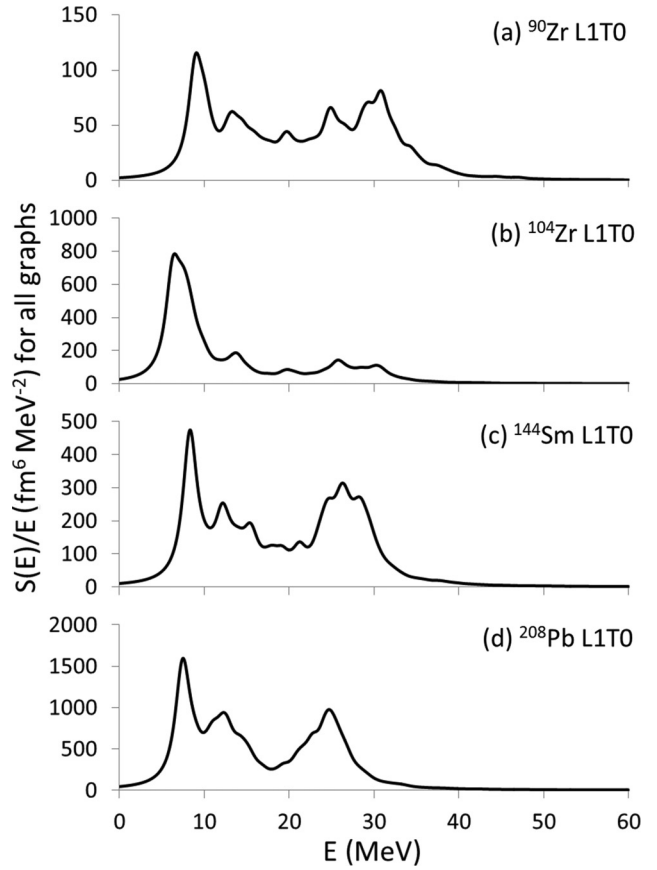

FIG. 6. Same as Fig. 5 but for the ^{90}Zr, ^{104}Zr, ^{144}Sm, and ^{208}Pb nuclei.

In Table I, we present the values of the centroid energies m_1/m_0 (in MeV) for the ISGDR, obtained by using the probing operator of Eqs. (6) and (15), and the OIVGDR, obtained by using the probing operator of Eqs. (7) and (15) for a wide range of nuclei. The KDE0v1 Skyrme interaction [25] was used in the calculations. The ISGDR and OIVGDR are calculated over the excitation energy ranges of 16–40 and 20–60 MeV, respectively.

In Table II, we display the HF-based RPA results for the inverse energy moment, m_{-1} of the ISD strength distribution, obtained by using the probing operator of Eqs. (6) and (15) and, for the IVD, obtained by using the probing operator of Eqs. (7) and (15) in ^{208}Pb, calculated for 18 frequently used Skyrme-type interactions (see Ref. [16]). Note that the values of inverse energy moment m_{-1} of the ISD are in the range of 14 000–20 000 fm^6 MeV^{-1} and the corresponding values for the IVD are only about 10%–12% of that of the ISGDR.

In Table III, we show the HF-based RPA results for the m_{-1} of the ISD, obtained by using the probing operator of Eqs. (6) and (15), and the IVD, obtained by using the probing operator of Eqs. (7) and (15) for the same nuclei shown in Table I. The KDE0v1 Skyrme interaction [25] was used in the calculations. Note the significant enhancement in the values of the inverse energy moment m_{-1} in neutron-rich isotopes, which is associated with the increase in the ISD and IVD strengths at low energy.

TABLE I. Values of the centroid energies m_1/m_0 (in MeV) for the ISGDR, obtained by using the probing operator of Eqs. (6) and (15), and the OIVGDR, obtained by using the probing operator of Eqs. (7) and (15), for a wide range of nuclei, calculated by using the KDE0v1 Skyrme interaction [25]. The ISGDR and OIVGDR are calculated over the excitation energy ranges of 16–40 and 20–60 MeV, respectively.

	ISGDR	OIVGDR
^{40}Ca	27.9	38.4
^{48}Ca	29.0	39.6
^{56}Ni	28.5	39.5
^{68}Ni	28.4	38.5
^{78}Ni	28.2	39.6
^{90}Zr	28.0	38.2
^{96}Zr	27.4	37.5
^{104}Zr	26.9	37.5
^{100}Sn	27.7	38.5
^{144}Sm	26.3	36.9
^{208}Pb	24.5	35.2

TABLE II. Valuesof m_{-1} (in fm^6 MeV^{-1}) for the ISD, obtained by using Eqs. (6) and (15), and for the IVD, obtained by using Eqs. (7) and (15) in ^{208}Pb for the following Skyrme interactions: SGII [24], KDE0 [25], KDE0v1 [25], SKM* [26], SK255 [27], SkI3 [28], SkI4 [28], SkI5 [28], SV-bas [29], SV-min [29], SV-m56-O [30], SV-m64-O [30], SLy4 [31], SLy5 [31], SLy6 [31], SkMP [32], SkP [33], and SkO′ [34]. The excitation energy range of 0–60 MeV was used.

^{208}Pb	$L1T0\ m_{-1}$	$L1T1\ m_{-1}$
SGII	17 233	1968
KDE0	17 752	1858
KDE0v1	17 737	1806
SKM*	18 758	1999
SK255	18 375	1926
SkI3	14 312	1771
SkI4	16 750	1678
SkI5	18 207	1909
SV-bas	17 386	1865
SV-min	18 525	1868
SV-m56-O	16 039	1561
SV-m64-O	16 299	1630
SLy4	17 501	1920
SLy5	17 422	1909
SLy6	17 650	1912
SkMP	18 409	1996
SkP	19 758	2020
SkO′	19 477	1937

By considering, for example, the case of ^{208}Pb, we find that the centroid energies of the ISGDR and the OIVGDR in ^{208}Pb are 24.5 and 35.2 MeV, respectively. The values of the inverse energy moment are $m_{-1} = 177\ 737$ and 1806 fm^6 MeV^{-1} for the ISD and the IVD in ^{208}Pb, respectively. The value of m_{-1} of the IVD is only about 10% of that of the ISD. The findings for this nucleus are consistent with the estimate found for the Schiff moment in Ref. [1]. By using the expressions for the weak interaction part from the above reference, we find that the contribution to the Schiff moment considered here is as large as the result obtained by using the single-particle models (see, for example, Ref. [35] and references therein).

IV. CONCLUSIONS

We have presented results of our fully self-consistent HF-RPA calculations by using 18 commonly employed Skyrme-type interactions [16] for the strength functions and corresponding inverse energy moments of the ISD and IVD for various nuclei by using a probing operator, which is the same as the Schiff operator up to a normalization. We have seen that the contribution of the IVD to the Schiff strength distribution in the even-even nucleus is smaller by an order of magnitude than that of the ISD. We find that, in exotic nuclei with large neutron excess, the ISD and the IVD strength distributions are pushed to lower energies and, thus, considerably increasing the inverse energy moment m_{-1} of the strength distribution. In particular, this means that the ISD contribution to the Schiff moment in the odd-even nucleus might be enhanced further. We also find that the contribution of the isovector inverse energy Schiff distribution in the even-even nucleus is smaller than that of the isoscalar by an order of magnitude.

TABLE III. Self-consistent HF-based RPA results for the inverse energy moment m_{-1} (fm^6 MeV^{-1}) of the ISD, obtained by using the probing operator of Eqs. (6) and (15), and of the IVD, obtained by using the probing operator of Eqs. (7) and (15) for a wide range of nuclei, calculated by using the KDE0v1 Skyrme interaction [25]. The excitation energy range of 0–60 MeV was used.

	$L1T0\ m_{-1}$	$L1T1\ m_{-1}$
^{40}Ca	332	53
^{48}Ca	499	67
^{56}Ni	491	76
^{68}Ni	1326	167
^{78}Ni	2030	203
^{90}Zr	1708	226
^{96}Zr	3630	465
^{104}Zr	6069	664
^{100}Sn	1988	269
^{144}Sm	5853	668
^{208}Pb	17 737	1806

The distributions of low-lying dipole strength (both isoscalar and isovector) presently are the subject of a large number of experimental studies. Our paper provides a theoretical description of these distributions for a wide range of nuclei. Moreover, the various studies in the past (except for Ref. [1]) have not addressed the question of the relation between the low-lying dipole strength and the Schiff moment, a quantity that is central to atomic studies of time-reversal violation [1,3,4,13,35]. This relation is emphasized strongly and is discussed extensively in this paper. Future experiments that will measure static electric dipole moments by using exotic atoms with large neutron excess spherical nuclei will need to use theoretical input to relate the results obtained to the limits of time-reversal conservation. The results of the present study will be of help in this respect.

ACKNOWLEDGMENTS

We thank V. Zelevinsky for helpful discussions. N.A. and C.S. wish to thank the Bulgarian and Israel National Academy of Science for their support of this project. S.S. thanks Tel-Aviv University for its kind hospitality. This work was supported, in part, by the U.S. Department of Energy under Grant No. DOE-FG03-93ER40773. C.S. acknowledges support of the Bulgarian Science Foundation under contract NuPNET-SARFENDNS7RP01/0003.

[1] N. Auerbach and V. Zelevinsky, Phys. Rev. C **86**, 045501 (2012).

[2] M. N. Harakeh and A. E. L. Dieperink, Phys. Rev. C **23**, 2329 (1981); N. Van Giai and H. Sagawa, Nucl. Phys. A **371**, 1 (1981).

[3] N. Auerbach, V. V. Flambaum, and V. Spevak, Phys. Rev. Lett. **76**, 4316 (1996).
[4] N. Auerbach and V. Zelevinsky, J. Phys. G **35**, 093101 (2008).
[5] H. P. Morsch, M. Rogge, P. Turek, and C. Mayer-Böricke, Phys. Rev. Lett. **45**, 337 (1980).
[6] D. H. Youngblood, Y.-W. Lui, H. L. Clark, B. John, Y. Tokimoto, and X. Chen, Phys. Rev. C **69**, 034315 (2004); D. H. Youngblood, Y.-W. Lui, B. John, Y. Tokimoto, H. L. Clark, and X. Chen, *ibid.* **69**, 054312 (2004).
[7] U. Garg, Nucl. Phys. A **731**, 3 (2004).
[8] A. P. Tonchev, S. L. Hammond, J. H. Kelley, E. Kwan, H. Lenske, G. Rusev, W. Tornow, and N. Tsoneva, Phys. Rev. Lett. **104**, 072501 (2010).
[9] J. Endres, D. Savran, P. A. Butler, M. N. Harakeh, S. Harissopulos, R.-D. Herzberg, R. Krücken, A. Lagoyannis, E. Litvinova, N. Pietralla, V. Yu Ponomarev, L. Popescu, P. Ring, M. Scheck, F. Schlüter, K. Sonnabend, V. I. Stoica, H. J. Wörtche, and A. Zilges, Phys. Rev. C **85**, 064331 (2012).
[10] V. G. Soloviev, C. Stoyanov, and V. V. Voronov, Nucl. Phys. A **304**, 503 (1978).
[11] N. Tsoneva, H. Lenske, and C. Stoyanov, Phys. Lett. B **586**, 213 (2004).
[12] J. Kvasil, V. O. Nesterenko, W. Kleinig, D. Bozik, P.-G. Reinhard, and N. Lo Iudice, Eur. Phys. J. A **49**, 119 (2013).
[13] W. C. Griffith, M. D. Swallows, T. H. Loftus, M. V. Romalis, B. R. Heckel, and E. N. Fortson, Phys. Rev. Lett. **102**, 101601 (2009).
[14] E. Chabanat, P. Bonche, P. Haensel, J. Meyer, and R. Schaeffer, Nucl. Phys. A **627**, 710 (1997).
[15] W. Kohn, Rev. Mod. Phys. **71**, 1253 (1999).
[16] M. R. Anders, S. Shlomo, T. Sil, D. H. Youngblood, Y.-W. Lui, and Krishichayan, Phys. Rev. C **87**, 024303 (2013).
[17] P.-G. Reinhardt, Ann. Phys. **1**, 632 (1992).
[18] T. Sil, S. Shlomo, B. K. Agrawal, and P.-G. Reinhard, Phys. Rev. C **73**, 034316 (2006).
[19] V. O. Nesterenko, J. Kvasil, and P.-G. Reinhard, Phys. Rev. C **66**, 044307 (2002).
[20] A. Bohr and B. M. Mottelson, *Nuclear Structure II* (Benjamin, New York, 1975).
[21] E. Lipparini and S. Stringari, Phys. Rep. **175**, 103 (1989).
[22] S. Shlomo and A. I. Sanzhur, Phys. Rev. C **65**, 044310 (2002).
[23] B. K. Agrawal, S. Shlomo, and A. I. Sanzhur, Phys. Rev. C **67**, 034314 (2003).
[24] N. Van Giai and H. Sagawa, Phys. Lett. B **106**, 379 (1981).
[25] B. K. Agrawal, S. Shlomo, and V. Kim Au, Phys. Rev. C **72**, 014310 (2005).
[26] J. Bartel, P. Quentin, M. Brack, C. Guet, and H. B. Hakansson, Nucl. Phys. A **382**, 79 (1986).
[27] B. K. Agrawal, S. Shlomo, and V. Kim Au, Phys. Rev. C **68**, 031304 (2003).
[28] P.-G. Reinhard and H. Flocard, Nucl. Phys. A **587**, 467 (1995).
[29] P. Klupfel, P.-G. Reinhard, T. J. Burvenich, and J. A. Maruhn, Phys. Rev. C **79**, 034310 (2009).
[30] N. Lyutorovich, V. I. Tselyaev, J. Speth, S. Krewald, F. Grümmer, and P.-G. Reinhard, Phys. Rev. Lett. **109**, 092502 (2012).
[31] E. Chabanat, P. Bonche, P. Haensel, J. Meyer, and R. Schaeffer, Nucl. Phys. A **635**, 231 (1998).
[32] L. Bennour, P.-H. Heenen, P. Bonche, J. Dobaczewski, and H. Flocard, Phys. Rev. C **40**, 2834 (1989).
[33] J. Dobaczewski, H. Flocard, and J. Treiner, Nucl. Phys. A **422**, 103 (1984).
[34] P.-G. Reinhard, D. J. Dean, W. Nazarewicz, J. Dobaczewski, J. A. Maruhn, and M. R. Strayer, Phys. Rev. C **60**, 014316 (1999).
[35] J. S. M. Ginges and V. V. Flambaum, Phys. Rep. **397**, 63 (2004).